NAVAL POSTGRADUATE SCHOOL

MONTEREY, CALIFORNIA

THESIS

ADVANCED RESEARCH INTO MOVING TARGET IMAGING USING MULTISTATIC RADAR

by

Grant H. Riedl

December 2009

Thesis Advisor:	Brett Borden
Second Reader:	Donald Walters

Approved for public release; distribution is unlimited

REPORT DOCUMENTATION PAGE — *Form Approved OMB No. 0704-0188*

1. AGENCY USE ONLY *(Leave blank)*	**2. REPORT DATE** December 2009	**3. REPORT TYPE AND DATES COVERED** Master's Thesis

4. TITLE AND SUBTITLE
Advanced Research into Moving Target Imaging Using Multistatic Radar

5. FUNDING NUMBERS

6. AUTHOR(S) Riedl, Grant H.

7. PERFORMING ORGANIZATION NAME(S) AND ADDRESS(ES)
Naval Postgraduate School
Monterey, CA 93943-5000

8. PERFORMING ORGANIZATION REPORT NUMBER

9. SPONSORING /MONITORING AGENCY NAME(S) AND ADDRESS(ES)
N/A

10. SPONSORING/MONITORING AGENCY REPORT NUMBER

11. SUPPLEMENTARY NOTES The views expressed in this thesis are those of the author and do not reflect the official policy or position of the Department of Defense or the U.S. Government.

12a. DISTRIBUTION / AVAILABILITY STATEMENT
Approved for public release: distribution is unlimited.

12b. DISTRIBUTION CODE

13. ABSTRACT (maximum 200 words)

Current active imaging algorithms for moving targets suffer from issues of incorrect positions (spatial) and streaking artifacts (temporal). Using the Cheney/Borden procedure, we investigated combining the spatial, temporal, and spectral aspects of real and synthetic aperture radar images. We code the Cheney/Borden algorithm to include the target velocity, include an appropriate threshold, and illustrate how multistatic radar can determine a target's location in phase space. By running simulations on single and multiple moving targets, we showed that an iteration of velocity and position choices for targets enhanced the correlation map for multistatic radar systems.

14. SUBJECT TERMS

Moving Target Imaging, Multistatic Radar, Computer Simulation

15. NUMBER OF PAGES
45

16. PRICE CODE

17. SECURITY CLASSIFICATION OF REPORT Unclassified	**18. SECURITY CLASSIFICATION OF THIS PAGE** Unclassified	**19. SECURITY CLASSIFICATION OF ABSTRACT** Unclassified	**20. LIMITATION OF ABSTRACT** UU

THIS PAGE INTENTIONALLY LEFT BLANK

ADVANCED RESEARCH INTO MOVING TARGET IMAGING USING MULTISTATIC RADAR

Grant H. Riedl
Lieutenant, United States Navy
B.S., University of Nebraska at Lincoln, 2002

Submitted in partial fulfillment of the
requirements for the degree of

MASTER OF SCIENCE IN APPLIED PHYSICS

from the

NAVAL POSTGRADUATE SCHOOL
December 2009

Author: Grant H. Riedl

Approved by: Prof. Brett Borden

Prof. Donald Walters

Prof. Andres Larraza
Chairman, Department of Physics

THIS PAGE INTENTIONALLY LEFT BLANK

ABSTRACT

Current active imaging algorithms for moving targets suffer from issues of incorrect positions (spatial) and streaking artifacts (temporal). Using the Cheney/Borden procedure, we investigated combining the spatial, temporal, and spectral aspects of real and synthetic aperture radar images. We code the Cheney/Borden algorithm to include the target velocity, include an appropriate threshold, and illustrate how multistatic radar can determine a target's location in phase space. By running simulations on single and multiple moving targets, we showed that an iteration of velocity and position choices for targets enhanced the correlation map for multistatic radar systems.

THIS PAGE INTENTIONALLY LEFT BLANK

TABLE OF CONTENTS

THIS PAGE INTENTIONALLY LEFT BLANK

LIST OF FIGURES

THIS PAGE INTENTIONALLY LEFT BLANK

I. INTRODUCTION

A. INTRODUCTION

This first chapter is an overview of the physicals foundations used in the simulations leading to synthetic aperture radar. This overview is presented as a foundation for Chapter II, which reviews previous work.

B. MAXWELL'S EQUATIONS

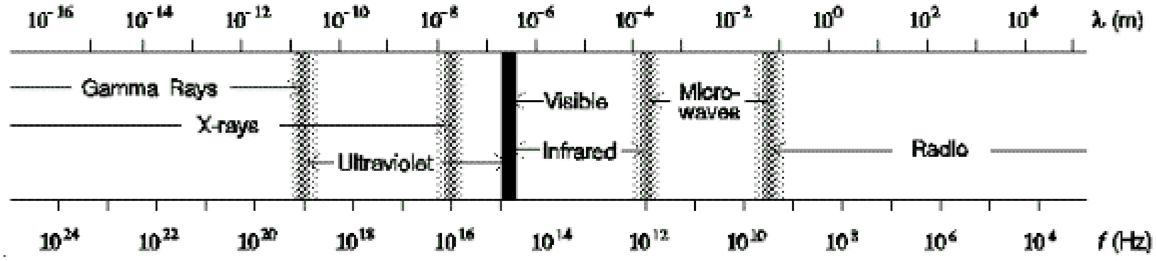

Figure 1. Electromagnetic spectrum (From [1])

Observations of the electromagnetic spectrum (Figure 1) and the associated Lorentz force law provided physicists with the building blocks required to explain the electromagnetic spectrum in terms of two fields. The fields are the Electric (E) and Magnetic (B) fields and they determine the forces felt by any charged object. In free space, monochromatic versions of each field travel in a sinusoidal pattern: they are perpendicular to each other and are in phase with each other. These observations led physicists to develop the building blocks for the Maxwell equations.

James Clerk Maxwell was known for many things, but his greatest accomplishment was completing and consolidating electro-magnetic theory. Maxwell realized that Gauss' law for Electricity,

$$\nabla \cdot D = \rho \tag{1.1}$$

where $D = \varepsilon E$, and ρ is the charge density, the equivalent law for magnetism

$$\nabla \cdot B = 0 \tag{1.2}$$

Faraday’s law,

$$\nabla \times E = -\frac{\partial B}{\partial t} \tag{1.3}$$

and Ampere’s law with Maxwell’s correction

$$\nabla \times H = J + \frac{\partial D}{\partial t} \tag{1.4}$$

where $H = B/\mu$, and by the inclusion of the displacement current J could be used to define the four fundamental laws of Electromagnetic theory, and the theory of light.

C. ELECTROMAGNETIC/RADAR THEORY

The principles of electromagnetic and radar theory rely on the Maxwell's equations. Radar theory is a practical expansion of the fundamental theory of electrodynamics and is implemented in many radar systems in use today.

1. Electromagnetic Theory

A key building block to electromagnetic theory is the electromagnetic wave equation. By simple mathematical manipulation Maxwell’s equations become inhomogeneous wave equations,

$$\nabla^2 B - \mu_0 \varepsilon_0 \frac{\partial^2 B}{\partial t^2} = -\mu \nabla \times j\ . \tag{1.5}$$

In free space they become the homogeneous wave equation.

$$\nabla^2 B - \mu_0 \varepsilon_0 \frac{\partial^2 B}{\partial t^2} = 0 \tag{1.6}$$

The same manipulations applying to the electric field give:

$$\nabla^2 E - \mu\varepsilon \frac{\partial^2 E}{\partial t^2} = \mu \frac{\partial J}{\partial t} + \frac{\nabla \rho}{\varepsilon} \tag{1.7}$$

These wave equations provide the basic foundation for numerous radar equations.

2. Radar Theory

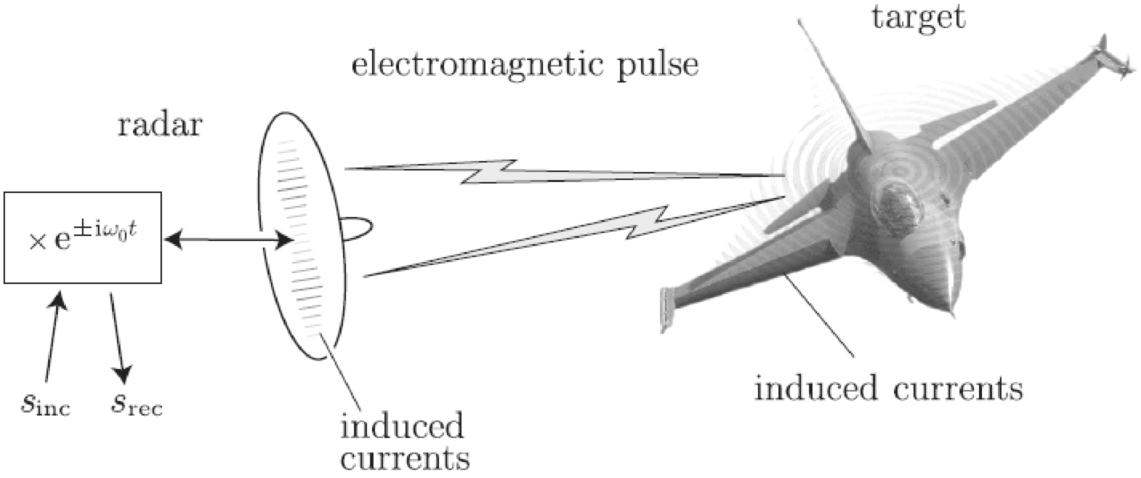

Figure 2. Basic radar system (From [2])

Figure 2 illustrates electric fields and currents induced on an antenna by a transmitter. Those fields produce an electromagnetic pulse that propagates through the medium and eventually interacts with a target. The electromagnetic pulse induces a current in the target, which in turn creates an electromagnetic pulse in response. This “scattered” electromagnetic pulse propagates back through the medium to the antenna where it induces a field. Using theories developed from the wave equations, the range can be determined from the signal resulting from the return field induced on the antenna.

D. RADAR RANGE-PROFILES

Current radars assume targets are effectively stationary. This is a good approximation since the duration of the pulses are relatively small and the speed of the targets are a small fraction of the speed of light. Range-profiles are one-dimensional high range resolution images of the target using the assumption targets are stationary. It is difficult to use range-profiles for target identification since all the scatterers located at the same distance from the receiver have the same time delay. A single range-profile will not be able to distinguish a cross-range structure.

E. MULTIPLE-LOOKS

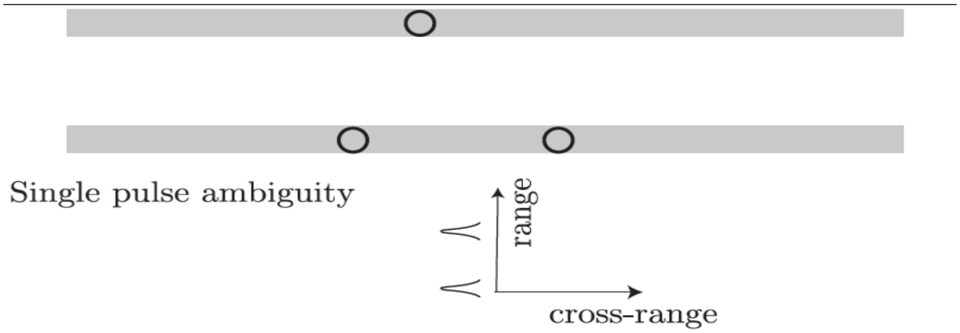

Figure 3. Single pulse ambiguity for targets of the same range (From [2])

Figure 3 illustrates how a single-range profile is not able to distinguish a cross-range structure of multiple targets at equal ranges.

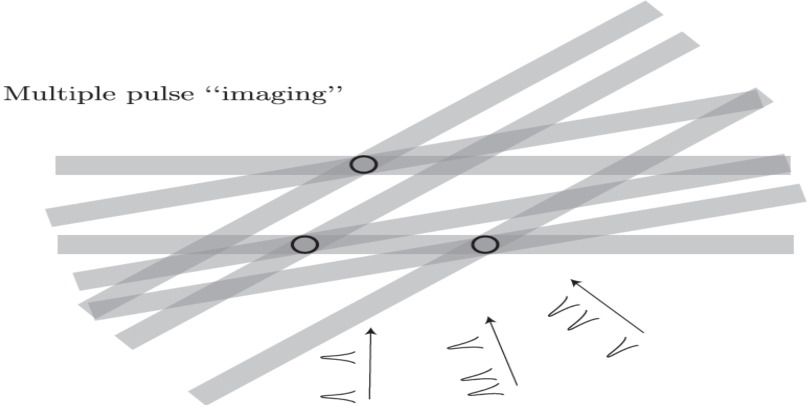

Figure 4. Multiple Pulse Radar (From [2])

A multiple pulse radar exploits multiple pulse data collected from multiple aspect angles to distinguish multiple targets that are at the same range. By applying the simple concept of triangulation, a multiple aspect radar is able to determine the range and cross-range of multiple targets. The multiple-look concept is a crude illustration of “filtered backprojection.”

F. FILTERED BACKPROJECTION

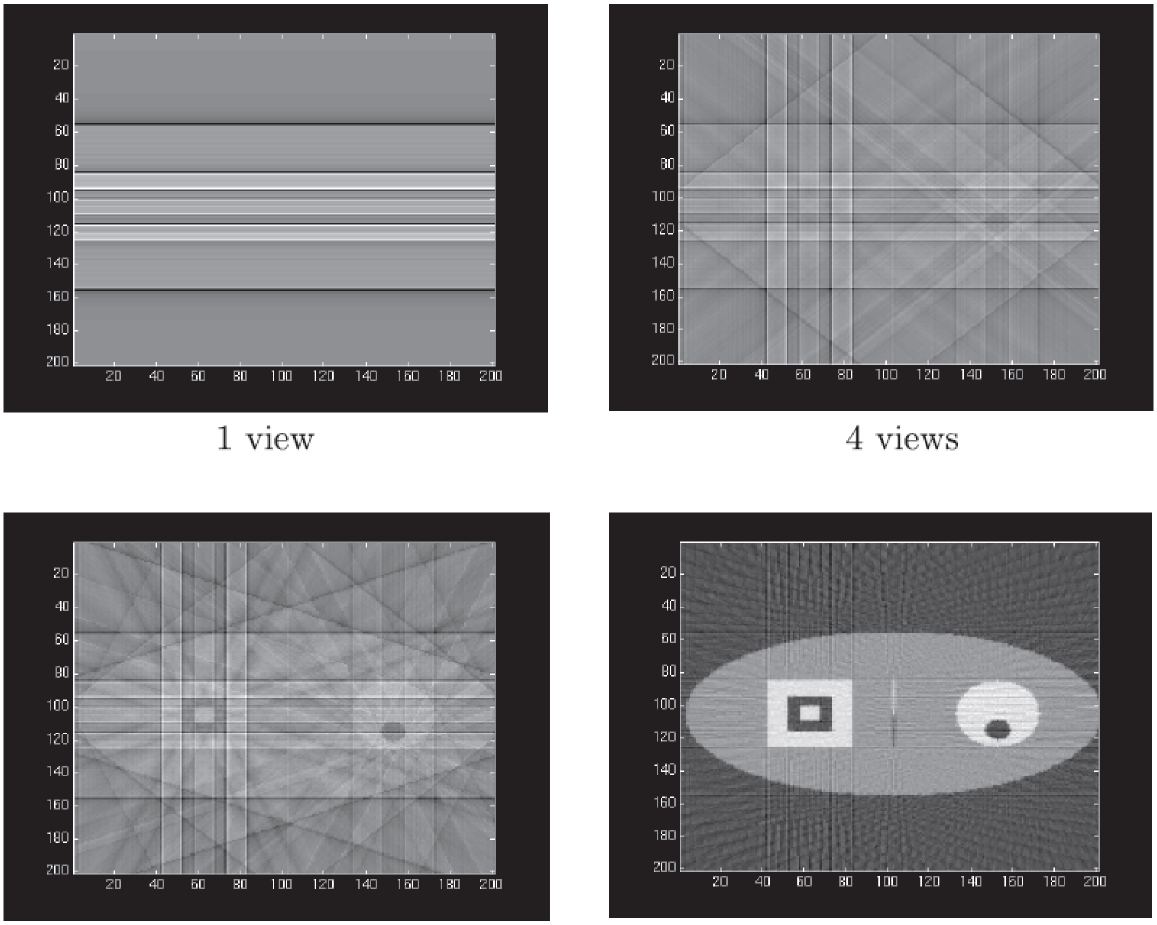

1 view

4 views

8 views

60 views

Figure 5. Filtered backprojection shown using single to multiple view angles (From [2])

Filtered backprojection takes multiple aspect radar range profiles, aligns them to a common origin, and sums the aligned data to produce an image of the scanned area. As the number of looks at multiple angles, in Figure 5, increases from 1 to 8, a discernable image starts to appear from the alignment and summation of the data. With 60 views at different angles, the filtered backprojection of the data displays a clear image. This provides a method to display multiple looks of data using the filtered backprojection method.

G. SYNTHETIC APERTURE IMAGING

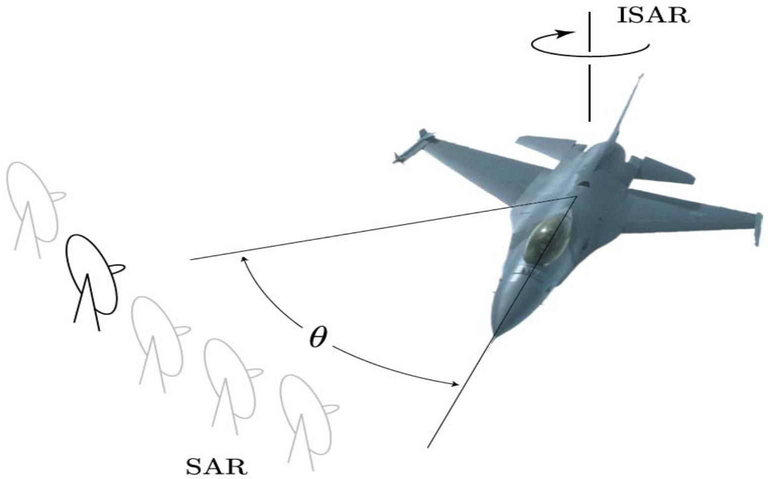

Figure 6. SAR and ISAR schemes for imaging targets (From [2])

Synthetic aperture imaging can be accomplished using a stationary antenna and rotating target or a stationary target with a moving antenna. Synthetic aperture radar (SAR) uses the concept of a moving antenna that illuminates a stationary target with a series of pulses from the moving antenna (Figure 6). Inverse synthetic aperture radar (ISAR) assumes a stationary radar radiating a moving target (Figure 6).

SAR imaging can be done either by tracking a single target of interest, known as spotlighting or by stripmapping.

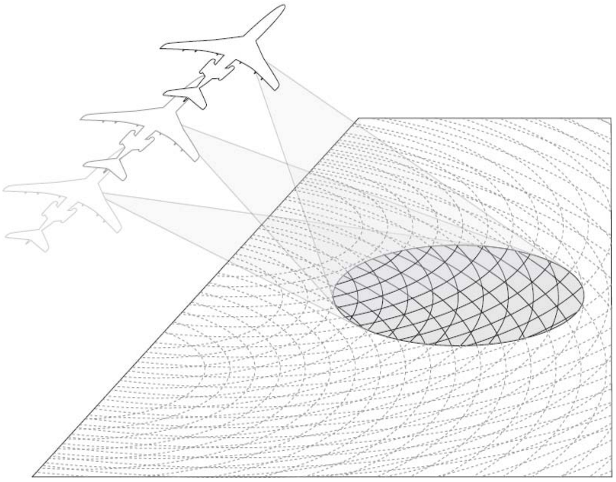

Figure 7. In spotlight SAR only one area is imaged (From [2])

In spotlight SAR a platform illuminates a specific area to get multiple images of the area from multiple aspect angles on the area. Spotlight SAR imaging is illustrated in Figure 7.

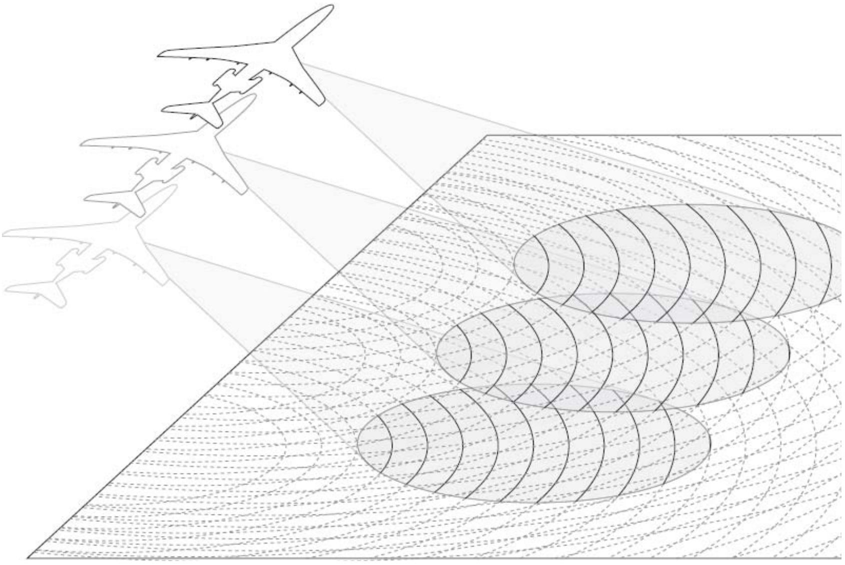

Figure 8. Stripmap SAR acquires a sequence of radar returns along a path (From [2])

Stripmap SAR requires a platform to sequentially illuminate a moving patch and then combines the measured returns to synthesize a larger image than typically available from spotlight SAR.

H. MOVING TARGETS

When a target moves, it rarely travels in a predictable manner. Unpredictable targets can cause problems with synthetic aperture radars because current SAR algorithms assume a stationary target. Moving targets add doppler frequency and phase shift artifacts. The most notable of problems is image artifacts. Image artifacts come from many sources: tank cannon barrels, jet engines, or (the most notable) the “train off the track” effect. The Cheney/Borden algorithm [3] does not assume a stationary target and, hopefully, images a moving train that is on the tracks.

THIS PAGE INTENTIONALLY LEFT BLANK

II. IMAGE ALGORITHM PROGRESSION

Chapter II will survey work previously completed, which will explain the chronology of developments of the Cheney/Borden algorithm.

A. THE CHENEY/BORDEN ALGORITHM

The Cheney/Borden Algorithm consists of a scattering model, imaging via a filtered adjoint, and image analysis.

1. Scattered Field for Moving Targets

Using the Born Approximation [4] for non-moving targets gives the scattered field as

$$\Psi_{scatt}\left(\vec{x},t\right) = \iiint\limits_{D} g\left(\vec{x}',\vec{x};t',t\right)\Psi_{inc}\left(\vec{x}',t'\right) d^3x' \,, \tag{2.1}$$

where $g\left(\vec{x}',\vec{x};t',t\right)$ is the time-domain Green function and $\Psi_{inc}\left(\vec{x}',t'\right)$ is the incident field. It can be shown[4] that when the incident field is formed using a time domain signal $s\left(t\right)$ transmitted from position y, that the scattering model becomes:

$$\psi_{scatt}\left(\vec{z},t\right) = \iint \frac{\delta\left(t-t'-\left|\vec{z}-\vec{x}'\right|/c\right)}{4\pi\left|\vec{z}-\vec{x}'\right|}\frac{\ddot{s}_y\left(t'+Ty-\left|\vec{x}'-\vec{y}\right|/c\right)}{4\pi\left|\vec{x}'-\vec{y}\right|}\rho\left(\vec{x}'\right)d^3x'dt' \,, \tag{2.2}$$

where $\rho\left(\vec{x}'\right)$ is the spatial scatterer density.

Tan Lu Pin and Teo Beng Koon William [4],[5],[6] have shown that a slowly moving target illuminated by a narrow-band waveform gives an approximate form for the scattered field of a moving target of the form:

$$\begin{aligned}\psi_{scatt}(\vec{y},\vec{z},t') \approx \frac{-\omega_y^2 e^{-i\omega_y t'}}{\left(4\pi\right)^2\left|\vec{z}\right|\left|\vec{y}\right|}\iint \exp\left\{-ik_y\left(\hat{y}-\hat{z}\right)\cdot\left[\vec{x}-\vec{v}\left(t'+\hat{z}\cdot\vec{x}/c\right)\right]\right\} \\ \times\tilde{s}_y\left(t'+\left(\hat{y}-\hat{z}\right)\cdot\vec{x}/c\right)\rho_v\left(x\right)d^3v d^3x \,.\end{aligned} \tag{2.3}$$

In this expression, we can ignore the constants in front of the integrand since they are not needed for imaging. Now, assuming the field is from an unknown point scatterer located at position p and velocity u, then Equation 2.3 reduces to [4]

$$\begin{aligned}\psi_{scatt}\left(\vec{y},\vec{z},t'\right)=-e^{-i\omega_y t'}\exp\left\{-ik_y\left(\hat{y}+\hat{z}\right)\cdot\left[\vec{p}-\vec{u}\left(t'-\hat{z}\cdot\vec{p}/c\right)\right]\right\}\\ \times\tilde{s}_y\left(t'+\left(\hat{y}+\hat{z}\right)\cdot\vec{p}/c\right)\ .\end{aligned} \tag{2.4}$$

The next step is to use the scattered and incident fields to create an imaging function.

2. Imaging via a Filtered Adjoint

Using the scattered field (Equation 2.2), a cross correlation gives an image of the form [4]

$$I\left(\vec{p},\vec{u}\right)=\iiint\psi_{scatt}\left(\vec{y},\vec{z},t'\right)\psi^*\left(\vec{y},\vec{z},t'\right)dt'd^m yd^n z\,, \tag{2.5}$$

where $m,n=1,2,3$ depending on the placement of the transmitters and receivers.

Because there is a chance of image artifacts for moving targets, we need to add a filtering function $Q\left(\omega,t',\vec{p},\vec{u},\vec{y},\vec{z}\right)$ so that [4]

$$I\left(\vec{p},\vec{u}\right)=\iiint\psi_{scatt}\left(\vec{y},\vec{z},t'\right)\psi^*\left(\vec{y},\vec{z},t'\right)Q\left(\omega,t',\vec{p},\vec{u},\vec{y},\vec{z}\right)dt'd^m yd^n z\,. \tag{2.6}$$

Expanding Equation 2.6, the imaging equation becomes [4]

$$\begin{aligned}I\left(\vec{p},\vec{u}\right)=-\iiint Q\left(\omega,t',\vec{p},\vec{u},\vec{y},\vec{z}\right)e^{i\omega_y t'}e^{ik_y\left(\hat{y}+\hat{z}\right)\cdot\left[\vec{p}-\vec{u}\left(t'+\vec{z}\cdot\vec{p}/c\right)\right]}\\ \times\tilde{s}_y\left(t'+\left(\hat{y}+\hat{z}\right)\cdot\vec{p}/c\right)\psi_{scatt}\left(\vec{y},\vec{z},t'\right)dt'd^m yd^n z\end{aligned} \tag{2.7}$$

Equation 2.7 forms the basis of an imaging algorithm.

3. Image Analysis

Choosing values of $Q\left(\omega,t',\vec{p},\vec{u},\vec{y},\vec{z}\right)$ that remove the $\left|\vec{z}\right|$ and $\left|\vec{y}\right|$ coordinates from the amplitude factor in Equation 2.3:

$$Q\left(\omega,t',\vec{p},\vec{u},\vec{y},\vec{z}\right)=\frac{(4\pi)\left|\vec{z}\right|\left|\vec{y}\right|}{\omega_y^2}\mathrm{J}\left(\vec{p},\vec{u},\hat{y},\hat{z}\right),$$

where $\mathrm{J}\left(\vec{p},\vec{u},\hat{y},\hat{z}\right)$ is a Jacobian introduced during the analysis. Equation 2.7 becomes [4]

$$I\left(\vec{p},\vec{u}\right)=\iint K\left(\vec{p},\vec{u},\hat{y},\hat{z}\right)\rho\left(\vec{x}\right)d^3v d^3x\,, \tag{2.8}$$

where $\rho\left(\vec{x}\right)$ represents a perfect/ideal image function, and [4]

$$\begin{aligned}K\left(\vec{p},\vec{u},\vec{y},\vec{z}\right)=\iint &\exp\left\{ik_y\left(\hat{y}+\hat{z}\right)\cdot\left[\vec{p}-\vec{x}-\vec{u}\left(\hat{z}\cdot\vec{p}\right)/c+\vec{v}\left(\hat{z}\cdot\vec{x}\right)/c\right]\right\}\\ &\times\int\tilde{s}_y^*\left(t'+\left(\hat{y}+\hat{z}\right)\cdot\vec{p}/c\right)\tilde{s}_y\left(t'+\left(\hat{y}+\hat{z}\right)\cdot\vec{x}/c\right)e^{-ik_y\left(\hat{y}+\hat{z}\right)\cdot\left(\vec{u}-\vec{v}\right)t'}dt'\\ &\times\mathrm{J}\left(\vec{p},\vec{u},\hat{y},\hat{z}\right)d^m y d^n z\end{aligned} \tag{2.9}$$

is the point spread function describing the image.

Making a change of variables, Equation 2.9 becomes [4],[5],[6]

$$\begin{aligned}K\left(\vec{p},\vec{u},\vec{y},\vec{z}\right)=\iint &\exp\left\{ik_y\left(\hat{y}+\hat{z}\right)\cdot\left[\vec{u}\left(\hat{z}\cdot\vec{p}\right)/c-\vec{v}\left(\hat{z}\cdot\vec{x}\right)/c\right]\right\}\\ &\times\exp\left\{ik_y\left(\hat{y}+\hat{z}\right)\cdot\left[\left(\vec{p}-\vec{x}\right)+\tfrac{1}{2}\left(\vec{u}-\vec{v}\right)\left(\hat{y}+\hat{z}\right)\cdot\left(\vec{p}+\vec{x}\right)\right]/c\right\}\\ &\times\chi\left(k_y\left(\hat{y}+\hat{z}\right)\cdot\left(\vec{u}-\vec{v}\right),\left(\hat{y}+\hat{z}\right)\cdot\left(\vec{p}-\vec{x}\right)/c\right)\mathrm{J}\left(\vec{p},\vec{u},\hat{y},\hat{z}\right)d^m y d^n z\ ,\end{aligned} \tag{2.10}$$

where χ is the radar ambiguity function

$$\chi\left(\nu,\tau\right)=\int_{-\infty}^{\infty}\tilde{s}_y^*\left(t+\tfrac{1}{2}\tau\right)\tilde{s}_y\left(t-\tfrac{1}{2}\tau\right)e^{-i\nu t}dt\,.$$

B. TAN LU PIN’S WORK

Tan Lu Pin (Tan) conducted simulations on the Cheney/Borden algorithm (Equation 2.8). Tan’s work showed that the imaging point spread function is well behaved, localizes the target in phase space and is translation invariant [6]. Phase space, in this context, is a space where position and velocity of an image point are represented, with correspond to one unique point in velocity and position space.

Localizing a target in phase space demonstrated that a moving target could be imaged in a multistatic environment in which target motion is not ignored. Tan examined a single point scatterer in a 2-D plane.

C. TEO BENG KOON WILLIAM'S WORK

Teo Beng Koon William (William) used the Cheney/Borden algorithm (Equation 2.8) to show that the scattering model, radar model, and imaging model could be combined. William ran simulations on each part and proved that for a single point scatterer a stationary target's location could be determined using a multistatic array [6].

III. DATA ANALYSIS

A. STRUCTURE

The current investigation was performed by Chee Young Ng, Christopher Carroll, and the author and started where Teo Beng Koon William concluded. Chapter III presents the chronology of work conducted utilizing the Cheney/Borden algorithm showing that for a single point scatterer a multistatic array can image a *moving* target.

B. CODING

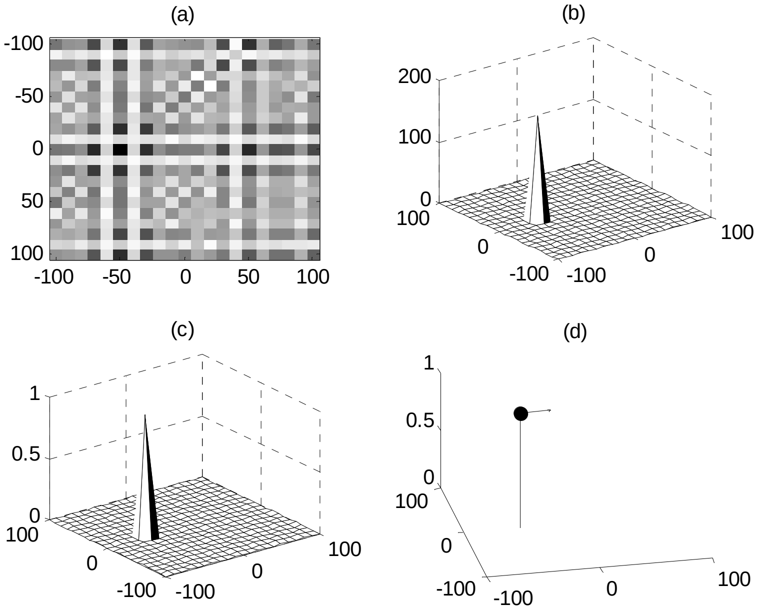

Figure 9. Display progressions of target located (-50,0)m with one transmitter located (-500,-500)m and four receiver located at (-500,-500)m, (-500,500)m, (500,500)m, (500,-500)m. (a) raw data (b) thresholded data (c) normalized data (d)stem/quiver plot of data. (x-y axis are in meters)

A Matlab code utilizing the Cheney/Borden algorithm appears in the Appendix. This code provided the basis for a series of simulation runs. The code has four parts. Including velocity and verifying imaging of a moving target was the driving force behind coding. Thresholding was needed to eliminate the image artifacts and thereby prevent false targets. Normalizing was used to display all velocities with the same peak value. Matlab was used to run simulations and display images created from the Cheney/Borden Algorithm.

1. Cheney/Borden Code

Up until now, the algorithm was run without considering target velocity and proved only that a point scatter could be located in space. Our first goal included velocity into a 2D code.

The Cheney/Borden algorithm produces an image by comparing the scattered field of a known target to the measured scattered field. The trial target's position and velocity must be specified with respect to each transmitter and receiver location. Cross-correlation forms the image. In our testing the Matlab code *imagesc* displays the correlation map (which constitutes the "image") (Figure 9a).

2. Thresholding

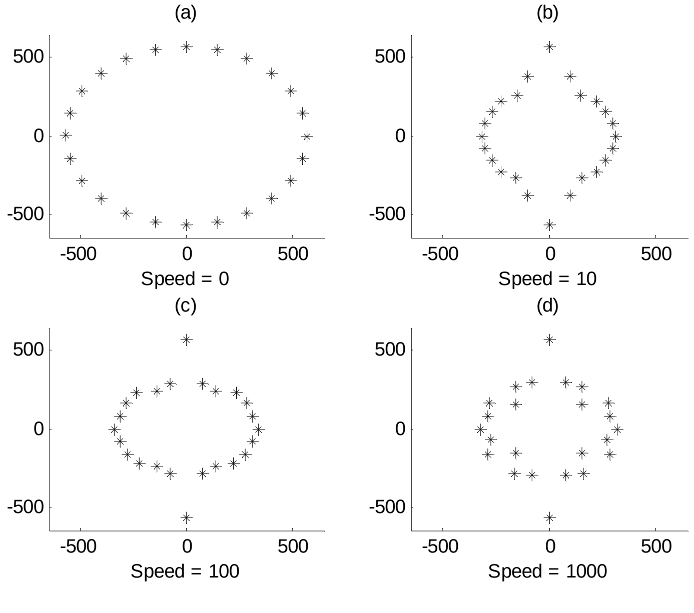

Figure 10. Max amplitude of velocity profiles at 15 degree cross-ranges

The peaks of the correlation map for stationary to slow moving targets were stronger than those of faster moving targets (Figure 10), causing the fast movers to be lost in the artifacts. The *imagesc* function in Matlab showed that the data needed to be thresholded to decrease the number of false returns (Figure 9a). The space, or lack thereof, around the target created the false artifacts.

Computing the minimum amplitude of velocity for a known target provided the threshold level. A conditional in the code set any computed point that fell below minimum amplitude for the given velocity to zero. By doing this, simulations with no targets moving at the checked velocities were set to zero. Figure 9b shows the data with a threshold partition. It is clear that the artifacts have been eliminated.

3. Normalization

After thresholding the correlation map image, amplitude normalization allows the imaging of multiple targets to be shown with the same peak level (Figure 9c). A partition in code allowed the data to be normalized for each velocity. Matlab code *imagesc* and *surf* displayed the data (Figure 9c).

4. Display

Finally, the imaged data needed to display the position, velocity and direction of the target. The ease of programming and graphing in Matlab made image display straightforward. The Matlab subroutine *imagesc* displays the data in a 2-D format, which provides the targets position. Matlab subroutine *surf* shows the intensity of the return from the imaged target in the form of a peak. The Matlab plot functions *stem* with *quiver* were the most intuitive with respect to a user-friendly display (Figure 9d).

THIS PAGE INTENTIONALLY LEFT BLANK

IV. FINDINGS AND FUTURE WORK

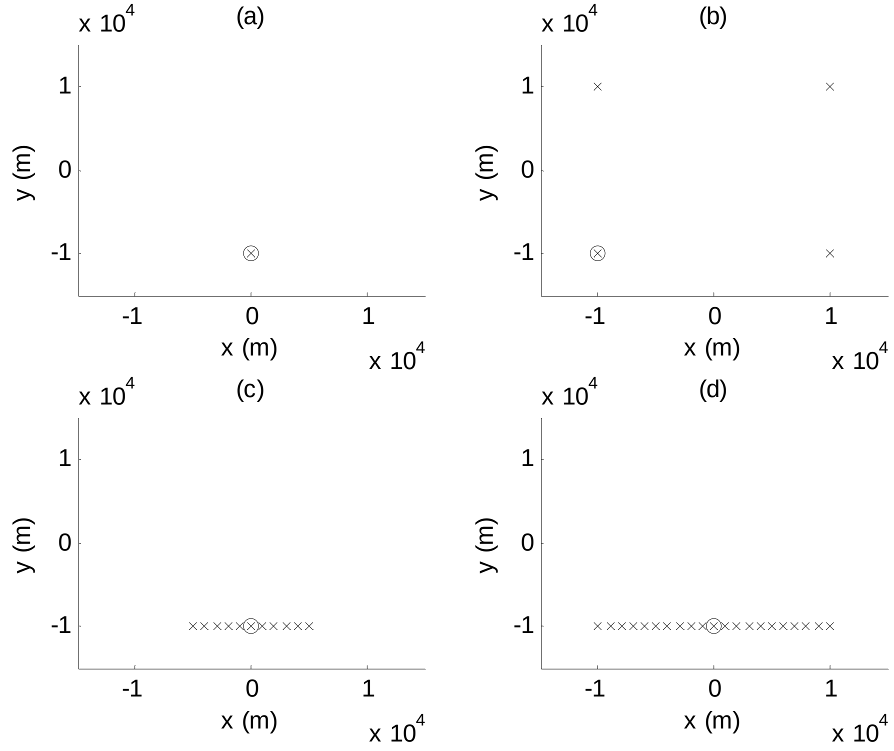

Figure 11. (a)One transmitter (O) and 1 receiver (X), (b) 1 transmitter and 4 receivers, (c) 1 transmitter and 11 receivers, (d) 1 transmitter and 21 receivers.

Simulations were run using both monostatic and multistatic configurations (see Figure 11). The transmitter and receivers were stationary for the simulations. The units in the x-y plane are in meters and the velocities in component form $\left(v_x, v_y\right)$, are in meters per second. The imaged area on the x-y plane is a square of dimension 200m x 200m centered at the origin (chosen to reduce Matlab computation time). A single pulse is of $0.2\mu s$ duration with a $100\mu s$ period. A pulse train is three $0.2\mu s$ pulses with a $100\mu s$ period.

A. FINDINGS

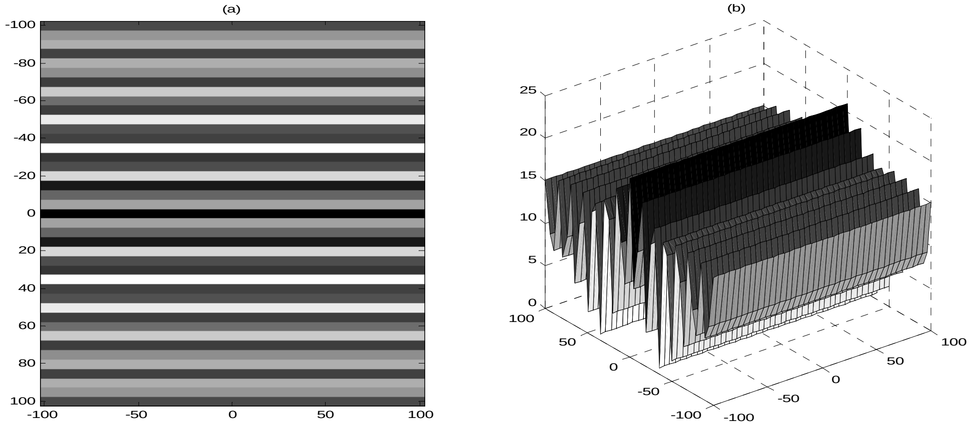

Figure 12. (a) *imagesc* and (b) *surf* display of single target, transmitter and receiver (x-y axis are in meters)

Figure 12a, illustrates an image formed from the sensor configuration of Figure 10a. The target was placed at (-50,0)m moving along the x-axis with velocity (10,0)m/s. A single pulse produces the correlation map of Figure 12 for a single transmitter and receiver this gives the range but not the cross-range location of the target.

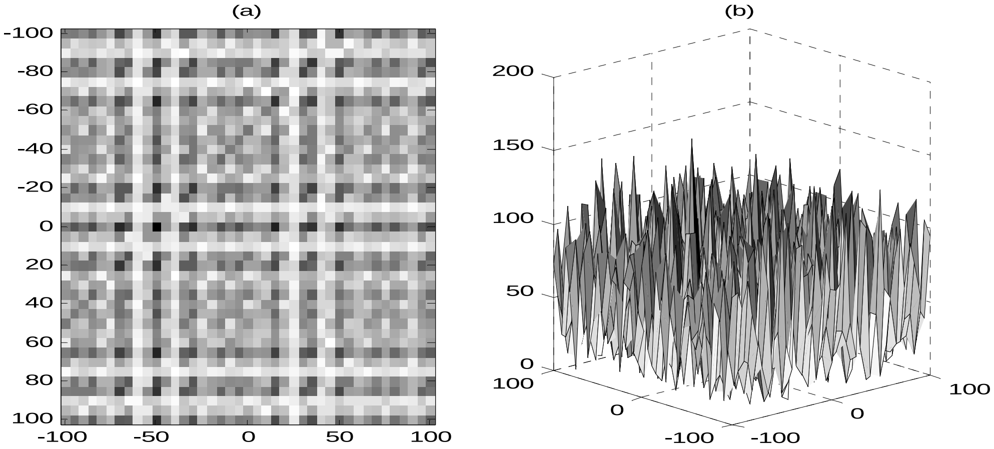

Figure 13. (a) *imagesc* and (b) *surf* display of 1transmiter and 4 receivers arranged as in Figure 11b (x-y axis are in meters)

The next imaging step added more receivers for a multistatic look at the area. A single pulse illuminated a target located at (-50,0)m with velocity (10,0)m/s. The transmitter and receiver setup was as in Figure 11b. Figure 13a shows an image of the target from the data, but there are image artifacts that confound image interpretation.

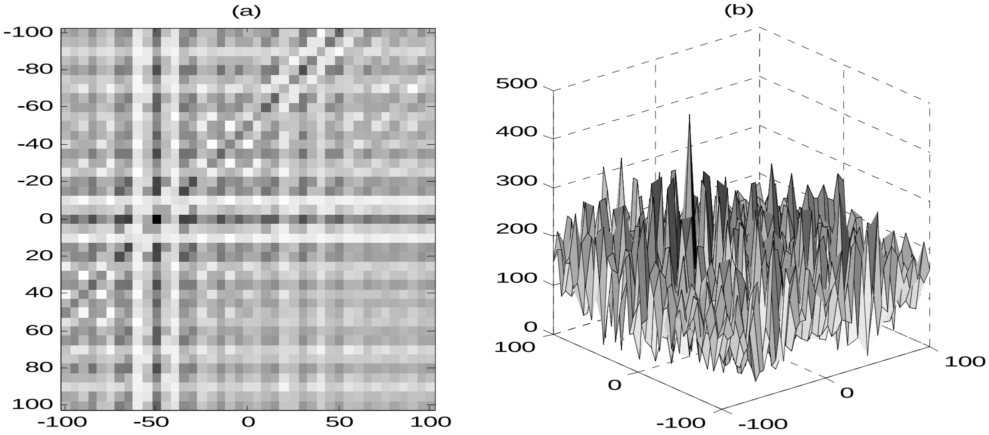

Figure 14. (a) *imagesc* and (b) *surf* display of 1transmiter and 4 receivers arranged as in Figure 11b (x-y axis are in meters)

The image in Figure 14 uses the same set-up for the target and receivers as in Figure 13. Figure 14 uses a pulse train for the image reducing the number of image artifacts.

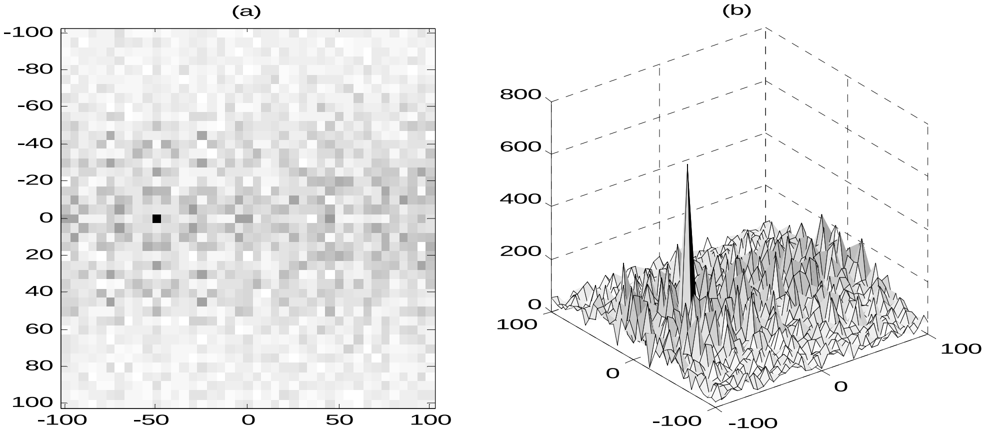

Figure 15. (a) *imagesc* and (b) *surf* display 1transmiter and 11 receivers arranged as in Figure 11c (x-y axis are in meters)

Figure 15 shows the target at (-50,0)m with a velocity of (10,0)m/s and imaged using a pulse train. Figure 15 shows that by increasing the number of receivers the image quality increases. Slower target speeds produce greater correlation peaks (Figure 15b).

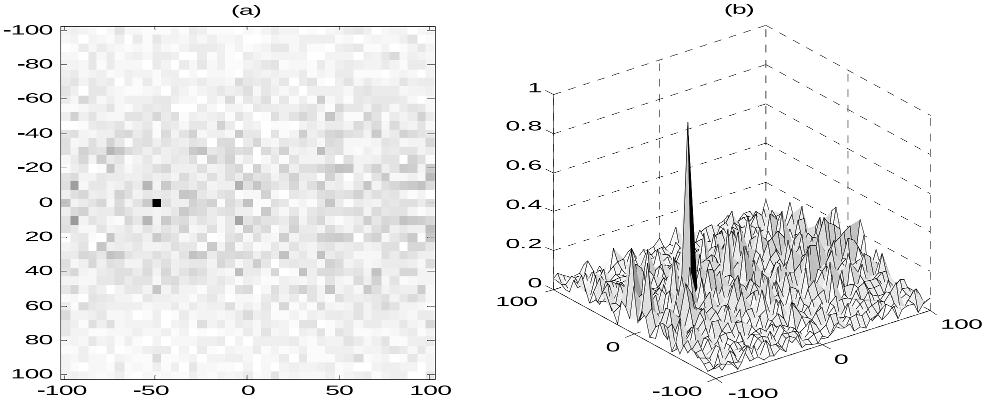

Figure 16. (a) *imagesc* and (b) *surf* normalized display 1transmiter and 21 receivers arranged as in Figure 11d (x-y axis are in meters)

Figure 16 reveals that increasing the number of receivers looking at an area produces a clearer image and reduces the image artifacts.

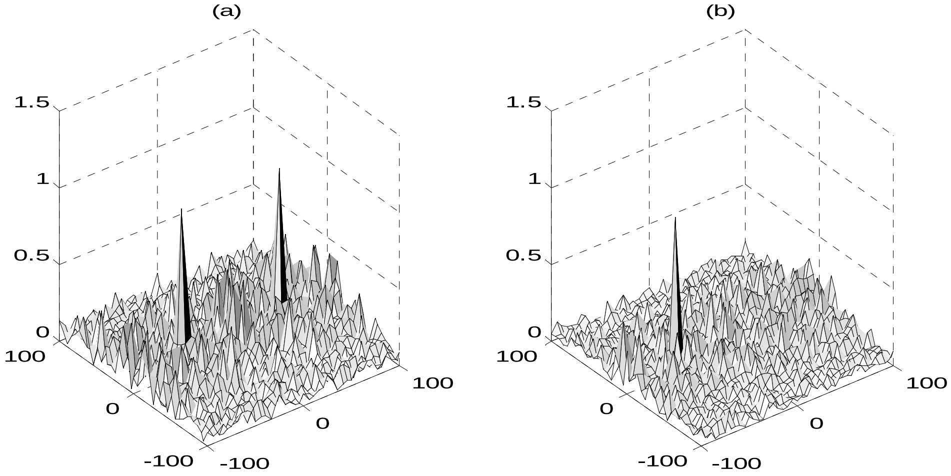

Figure 17. (a) & (b) *surf* plots of the same targets where (a) has targets of equal velocity, (b) has one target velocity significantly greater than the other (x-y axis are in meters)

Figure 17 incorporates targets with different velocities. Figure 17a has targets located at (-50,0)m, (50,0)m with a velocities of (10,0)m/s, (-10,0)m/s respectfully, and Figure 17b has targets at (-50,0)m,(50,0)m with velocities (-10,0)m/s,(-100,0)m/s respectfully. When the targets move at different velocities but near the same speed (Figure 17a), the peaks are well above the artifacts. Figure 17b shows that for significantly different speeds greater than a factor of 10, the faster target is lost in the artifacts. It was observed that thresholding would be required to see multiple targets moving at significantly different speeds. Thresholding would also be needed to remove the image artifacts from a correlation map with no target moving at the velocity used to compute the algorithm (from Chapter III).

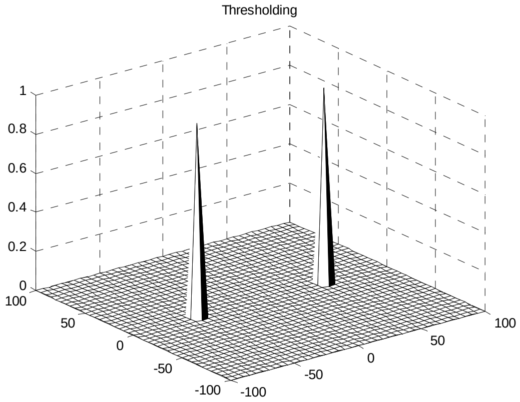

Figure 18. Multiple targets with a threshold applied, at significantly different velocities (x-y axis are in meters)

Figure 18 displays the thresholded version of the data used in Figure 17. The thresholding was done by inserting a loop into Matlab and a peak conditional that found the peak of the signal and removed the artifacts by setting a limit that an expected peak must exceed. When the data was summed and normalized, both peaks remained resulting in the image of the positions for each target.

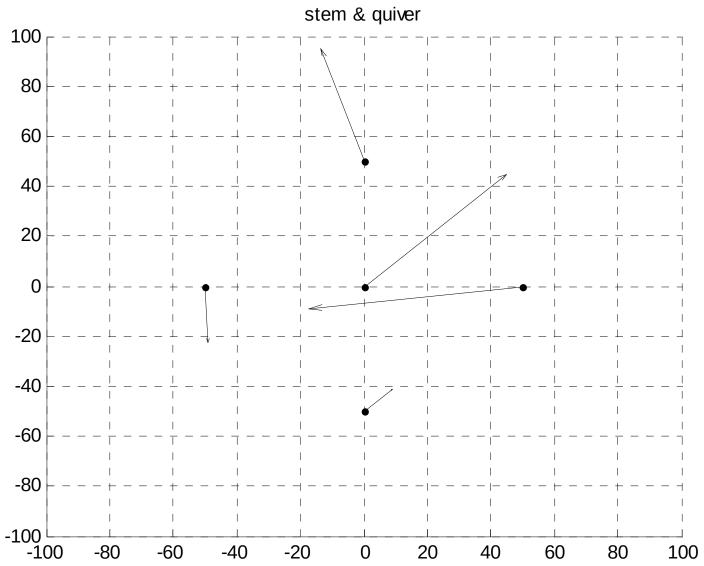

Figure 19. Plot of five targets using Matlab *stem* and *quiver* located (0,0)m, (50,50)m, (50,-50)m, (-50,50)m, (-50,-50)m with different velocities (x-y axis are in meters)

Figure 19 illustrates that the algorithm can distinguish multiple targets moving at multiple velocities in 2-D space. There were five targets moving with different velocities with the transmitter and receivers setup as in Figure 10d for this simulation. The Cheney/Borden algorithm was run with the image being produced by the Matlab codes *stem* and *quiver*. *Stem* provided the location of the target while *quiver* produced the velocity magnitude arrows. Using this setup a user would be able to see where the target is located and what velocity it has.

The targets for Figure 19 are point targets in a 2-D world. For actual data targets, the data would be a grouping of points with arrows from each point pointing in the same general direction.

B. FUTURE WORK

Future work on the project will be in five areas. The first area is in the speed at which the program runs. Matlab is a user-friendly interface that is easy to use but is it slow. Each simulation run took on average 40+ minuets to run. Taking the code and programming it into C as a .mex file to be called by Matlab would greatly increase the speed of the program. A faster program would greatly increase the number of simulations that could be run in a given day.

Being able to run more simulations would allow more display options to be considered. Displaying the data in a user-friendly manner is essential if anyone other than someone familiar with the code is to interpret it.

In principle, the fast-slow velocity correlations should be of the same magnitude, independent of velocities. We suspect that poor resolution produces poor correlation for larger velocities. Solving the correlation issues for large velocities should provide a better threshold value.

A big step in the progress of the project is to apply the algorithm to real data. Procuring unclassified data with which to run simulations is vital. Obtaining such data is one step of this project, while another step would be in assimilating the data into something that could be run with the algorithm.

While running the algorithm an appropriate form for the filtering function $Q\left(\omega,t',\vec{p},\vec{u},\vec{y},\vec{z}\right)$ is needed. For the current project, the filtering function used 1 in Equation 2.7 for expedience.   Depending on the medium and time of travel, the algorithm will need to be run multiple times to determine a best fit filtering function, bringing up the subject again of needing a faster way to run the algorithm.

THIS PAGE INTENTIONALLY LEFT BLANK

V. SUMMARY AND CONCLUSION

A. SUMMARY

In this thesis, we found that the Cheney/Borden algorithm could image a moving target and reduce the image artifacts associated with moving target images. It was found that each time the algorithm was run for a specified velocity, the targets moving at that velocity, could stand out in the displayed image. For a specified range of velocities, the program can be restricted to consider only targets falling within that velocity range for imaging purposes. For example, for images on the ground a vehicle, boat, or other target on the ground should not be moving faster than 70 miles per hour. The program can restrict target images to objects between 0 to 70 miles per hour. Constraining the velocity space will allow the images to be created faster allowing for faster review of the images.

B. CONCLUSION

The Cheney/Borden algorithm is a tool that incorporates the spatial, temporal and spectral aspects of radar returns into one equation. By combining these three aspects, multiple radar systems may no longer be required to image an area. Being able to image an object while simultaneously determining its position, heading, and velocity will revolutionize the radar community. The project is one step closer by confirming that a multistatic array can image an area and determine the position and velocity of multiple moving targets.

THIS PAGE INTENTIONALLY LEFT BLANK

APPENDIX

The Cheney/Borden algorithm was coded in Matlab, and shows how normalizing, thresholding, and displaying of the data is preformed to provide an image of the type in Chapters IV and V.

```
%Origin of the image scene is set at (0,0)
%Target Information
N_tt=1;                                   %No of Targets
tt=[-50 0;50 0];              %Target X - Y postion
tt_vel=[1 -25;-75 -10];       %Target velocity in X - Y direction

%Transmitter Information
N_Tx=1;                 %No of Transmitter
Tx =[0 -10e3];    %Transmitter X position, Y position
T_tx=0;                 %Start time of transmitted pulse
Tx_mag= sqrt(Tx(1,1)^2+Tx(1,2)^2);
Tx_hat = Tx/sqrt(Tx(1,1)^2+Tx(1,2)^2);

%Receiver Information
N_Rx=21;    %number of receivers
Rx=[-10e3 -10e3;-9e3 -10e3;-8e3 -10e3;-7e3 -10e3;-6e3 -10e3;-5e3 -
10e3;-4e3 -10e3;-3e3 -10e3;-2e3 -10e3;-1e3 -10e3;0 -10e3;1e3 -10e3;2e3
-10e3;3e3 -10e3;4e3 -10e3;5e3 -10e3;6e3 -10e3;7e3 -10e3;8e3 -10e3;9e3 -
10e3;10e3 -10e3];    %Receiver X - Y position
Rx_mag= sqrt(Rx(:,1).*Rx(:,1)+Rx(:,2).*Rx(:,2));
Rx_hat(:,1)=Rx(:,1)./sqrt(Rx(:,1).*Rx(:,1)+Rx(:,2).*Rx(:,2));
Rx_hat(:,2)= Rx(:,2)./sqrt(Rx(:,1).*Rx(:,1)+Rx(:,2).*Rx(:,2));

%Signal information
c=3e8;
W_tx=2*pi*(10e9);       %Carrier Freq is 10GHz
K_tx=W_tx/c;

%Waveform information
fs = 20e6;
t1 = 0:1:20;                  %pusle transmit time
t2 = 0:1:1979;                %listening time
period = 100e-6;
T_period=0:ts:100e-6;
T=[t1 t2 t1 t2 t1 t2];        %period of 100us
y = rectpuls(0,t1);
s = [y, zeros(1,length(t2))];
sp = [s s s];
S=fft(sp);        %FFT of signal
w=(2*pi/period)*T;
TT_Data=zeros(1,length(sp));

%Generating Target Signal
for l=1:N_Tx                  %For all Transmitter
    for m=1:N_Rx                    %For all Receiver
```

```
        for n=1:N_tt                %For all targets
            tau= T_tx+(((Tx_mag(l,:)-
(Tx_hat(l,:)*tt(n,:)’))+(Rx_mag(m,:)-(Rx_hat(m,:)*tt(n,:)’)))/c);
      %time delay
            phi=K_tx*Rx_mag(m,:)-
K_tx*(Tx_hat(l,:)+Rx_hat(m,:))*(tt(n,:)+((Rx_hat(m,:)*(Rx(m,:)-
tt(n,:))’)*tt_vel(n,:)/c))’;
            alpha=1-(Tx_hat(l,:)+Rx_hat(m,:))*(tt_vel(n,:)/c)’;
            TT_Data = TT_Data +
exp(i*phi)*exp(i*W_tx*alpha*T).*ifft(S.*exp(-i*w*tau));
        end;  end;  end
%Expected Target Position
E_tt_x=-1e2:5:1e2;            %Sampled by Range Resolution
E_tt_y=-1e2:5:1e2;            %Sampled by Range Resolution
E_tt_y=fliplr(E_tt_y);
%First speed
%Expected Target Velocity
for x = 1:N_tt                   %used for speed calculation
    for y = -200:200             %speed of target in x direction
        for z = -200:200         %speed of target in y direction
            if [tt_vel(x,1) tt_vel(x,2)] == [y z]
                V = sqrt(y^2+z^2);
            if V >= 0                     %function to find speed of
                  if V < 50               %target falls in range
E_tt_vel_x= y;
E_tt_vel_y= z;
E_tt_vel_y=fliplr(E_tt_vel_y);
E_tt_vel=[E_tt_vel_x E_tt_vel_y];

%%first speed
%Generating Expected Target Database
for g=1:length(E_tt_y)
    for h=1:length(E_tt_x)
        E_tt=[E_tt_x(1,h) E_tt_y(1,g)];
        E_TT_Data=zeros(1,length(T));
        for l=1:N_Tx                      %For all Transmitter
            for m=1:N_Rx                  %For all Receiver
                tau= T_tx+(((Tx_mag(l,:)-
(Tx_hat(l,:)*E_tt(1,:)’))+(Rx_mag(m,:)-(Rx_hat(m,:)*E_tt(1,:)’)))/c);
      %time delay
                phi=K_tx*Rx_mag(m,:)-
K_tx*(Tx_hat(l,:)+Rx_hat(m,:))*(E_tt(1,:)+((Rx_hat(m,:)*(Rx(m,:)-
E_tt(1,:))’)*E_tt_vel/c))’;
                alpha=1-(Tx_hat(l,:)+Rx_hat(m,:))*(E_tt_vel/c)’;
                E_TT_Data = E_TT_Data +
exp(i*phi)*exp(i*W_tx*alpha*T).*ifft(S.*exp(-i*w*tau));
            end;  end
        I(g,h)=E_TT_Data*TT_Data’;
    end;  end
for n = 1:length(E_tt_x)      %Thresholding
    for m = 1:length(E_tt_y)
        if C(n,m) >= 250
            D(n,m) = C(n,m);
        end
        if C(n,m) < 250
```

```
                j=0;
                D(n,m) = j;
end;  end;  end
A = max(max(abs(D)));   %largest value in D used for normalization
B = D./A;
C = abs(B);             %Normalized data
for n = 1:length(E_tt_x)
    for m = 1:length(E_tt_y)
        if D(n,m) >= 0.9
            H(1,1) = E_tt_x(1,m);
            H(1,2) = E_tt_y(1,n);
            H(1,3) = 0;
        end;  end;  end
stem3(H(1,1),H(1,2),H(1,3),’.k’)          %image of data created
quiver3(H(1,1),H(1,2),H(1,3),y,z,0,’k’)
axis([-100 100 -100 100 0 1])
grid
                    end;  end;  end;  end;  end;  end

%%%%%%%%%%%%%%%%%%%%%%%%%%%%%%%%%%%%%
%The following is an example of how the data could be partitioned for
%multiple velocities
%%%%%%%%%%%%%%%%%%%%%%%%%%%%%%%%%%%%%

%Second Speed
%%Expected Target Velocity
for x = 1:N_tt                        %used for speed calculation
    for y = -200:200                  %speed of target in x direction
        for z = -200:200              %speed of target in y direction
            if [tt_vel(x,1) tt_vel(x,2)] == [y z]
                V = sqrt(y^2+z^2);
                if V >= 50
                    if V < 100
E_tt_vel_x= y;
E_tt_vel_y= z;
E_tt_vel_y=fliplr(E_tt_vel_y);
E_tt_vel=[E_tt_vel_x E_tt_vel_y];

%Generating Expected Target Database
for g=1:length(E_tt_y)
    for h=1:length(E_tt_x)
        E_tt=[E_tt_x(1,h) E_tt_y(1,g)];
        E_TT_Data=zeros(1,length(T));
        for l=1:N_Tx                          %For all Transmitter
            for m=1:N_Rx                      %For all Receiver
                tau= T_tx+(((Tx_mag(l,:)-
(Tx_hat(l,:)*E_tt(1,:)’))+(Rx_mag(m,:)-(Rx_hat(m,:)*E_tt(1,:)’)))/c);
      %time delay
                phi=K_tx*Rx_mag(m,:)-
K_tx*(Tx_hat(l,:)+Rx_hat(m,:))*(E_tt(1,:)+((Rx_hat(m,:)*(Rx(m,:)-
E_tt(1,:))’)*E_tt_vel/c))’;
                alpha=1-(Tx_hat(l,:)+Rx_hat(m,:))*(E_tt_vel/c)’;
                E_TT_Data = E_TT_Data +
exp(i*phi)*exp(i*W_tx*alpha*T).*ifft(S.*exp(-i*w*tau));
            end;  end
        I(g,h)=E_TT_Data*TT_Data’;
    end;  end
for n = 1:length(E_tt_x)
    for m = 1:length(E_tt_y)
        if C(n,m) >= 160
            D(n,m) = C(n,m);
        end
        if C(n,m) < 160
            j=0;
            D(n,m) = j;
        end;  end;  end
A = max(max(abs(D)));
B = D./A;
C = abs(B);
for n = 1:length(E_tt_x)
    for m = 1:length(E_tt_y)
        if D(n,m) >= 0.9
            H(1,1) = E_tt_x(1,m);
            H(1,2) = E_tt_y(1,n);
            H(1,3) = 0;
        end;  end;  end
stem3(H(1,1),H(1,2),H(1,3),’.k’)
quiver3(H(1,1),H(1,2),H(1,3),y,z,0,’k’)
axis([-100 100 -100 100 0 1])
grid
                    end;  end;  end;  end;  end;  end
```

LIST OF REFERENCES

[1] "Theory of Synthetic Aperture Radar." Atlantis Scientific Inc. 1997. Retrieved from http://www.geo.unizh.ch/~fpaul/sar_theory.html on November 2, 2009.

[2] B. Borden. "Radar." Physics Department, Naval Postgraduate School, May 26, 2009.

[3] M. Cheney and B. Borden. "Imaging moving targets from scattered waves." IOP Publishing. April 8, 2008.

[4] B. Borden. "Moving Targets." Physics Department, Naval Postgraduate School, May 19, 2008.

[5] T. Lu Pin. "Analysis of Point-Spread Function for Imaging Moving Targets From Scattered Wave." Master's thesis, Naval Postgraduate School, 2008.

[6] T. Bing Koon William. "Radar Imaging for Moving Targets." Master's thesis, Naval Postgraduate School, 2009.

THIS PAGE INTENTIONALLY LEFT BLANK

INITIAL DISTRIBUTION LIST

1. Defense Technical Information Center
   Ft. Belvoir, Virginia

2. Dudley Knox Library
   Naval Postgraduate School
   Monterey, California

3. Grant H. Riedl
   Naval Postgraduate School
   Monterey, California